yielding 0·606, 0·030, 0·167 for n_0, n_1, n_2, respectively (with constraints $n_3 = n_2$, $n_4 = n_1$). These values suggest another type of disorder in this commensurate phase: inside large domains taken as reference ($T0$), there are smaller domains translated by $T2$ or $T3$ occupying 33% of the volume, and a small amount of domains translated by $T1$ and $T4$. The near absence of $T1$ and $T4$ domains can be interpreted by the fact that they cause much more perturbations at the domain walls. An example of a $T3$ domain is outlined in Fig. 7. It should be noted that these domains do not alter the global composition. We think that this kind of translated domain must be added to the tooth-like model for a complete description of most compounds in the range 1·0–1·33.

We think the domains found in $Ba_{1\cdot2}Ti_{6\cdot8}Mg_{1\cdot2}O_{16}$ could be explained by the fact that domain walls are pinned by inhomogeneities of the Ti/Mg distribution in the framework. In the study of $BaRu_6O_{12}$ (Torardi, 1985), the domain problem did not seem to arise; we suggest that its absence is due to the mixed-valence character of the framework cation Ru.

BG interpret the ionic conductivity by a displacement of domain walls, that is a collective movement of Ba^{2+} ions. A pinning of the domain walls on Ti/Mg inhomogeneities would obviously result in poor conductivity. The disorder problem has been addressed differently in the absence of three-dimensional correlations. Beyeler, Pietronero & Strässler (1980) use a short-range-order model to calculate diffuse profiles in $K_{1\cdot54}Ti_{7\cdot23}Mg_{0\cdot77}O_{16}$ and estimate the correlation length to be about 35 Å along the tunnel axis.

The authors greatly thank Dr F. de Bergevin for helpful comments, and acknowledge the skilful assistance of M. T. Roux in the crystal growth.

The X-ray data were collected within the 'Groupe Grenoblois de Diffractométrie'.

References

BEYELER, H. U., PIETRONERO, L. & STRÄSSLER, S. (1980). *Phys. Rev. B*, **22**, 2988-3000.
BEYELER, H. U. & SCHÜLER, C. (1980). *Solid State Ionics*, **1**, 77-86.
BURSILL, L. A. & GRZINIC, G. (1980). *Acta Cryst.* B**36**, 2902-2913.
BYSTRÖM, A. & BYSTRÖM, A. M. (1950). *Acta Cryst.* **3**, 146-154.
CHANG, F. M. & JANSEN, M. (1986). *Rev. Chim. Minér.* **23**, 48-54.
CHEARY, R. W. (1986). *Acta Cryst.* B**42**, 229-236.
COWLEY, J. M. & MOODIE, A. F. (1957). *Acta Cryst* **10**, 609-619.
DRYDEN, J. S. & WADSLEY, A. D. (1958). *Trans. Faraday Soc.* **54**, 1574-1580.
Enraf-Nonius (1979). *Structure Determination Package*. Enraf-Nonius, Delft, The Netherlands.
FANCHON, E., VICAT, J. & HODEAU, J.-L. (1987). In preparation.
HODEAU, J.-L., MAREZIO, M., SANTORO, A. & ROTH, R. S. (1983). *Solid State Ionics*, **9** & **10**, 77-82.
International Tables for X-ray Crystallography (1974). Vol. IV. Birmingham: Kynoch Press. (Present distributor D. Reidel, Dordrecht, The Netherlands.)
MIJLHOFF, F. C., IJDO, D. J. & ZANDBERGEN, H. W. (1985). *Acta Cryst.* B**41**, 98-101.
O'KEEFE, M. A. (1980). *SHRLI80F* (*Simulated High-Resolution Lattice Image*) programs. Univ. of Cambridge, England.
POST, J. E., VON DREELE, R. B. & BUSECK, P. R. (1982). *Acta Cryst.* B**38**, 1056-1065.
PRING, A., SMITH, D. J. & JEFFERSON, D. A. (1983). *J. Solid State Chem.* **46**, 373-381.
SHANNON, R. D. (1976). *Acta Cryst* A**32**, 751-767.
TORARDI, C. C. (1985). *Mater. Res. Bull.* **20**, 705-713.
VICAT, J., FANCHON, E., STROBEL, P. & TRAN QUI, D. (1986). *Acta Cryst.* B**42**, 162-167.
WATELET, H., BESSE, J.-P., BAUD, G. & CHEVALIER, R. (1982). *Mater. Res. Bull.* **17**, 863-871.
WEBER, H.-P. & SCHULZ, H. (1983). *Solid State Ionics*, **9** & **10** 1337-1340.
WOLFERS, P. (1987). In preparation.

Acta Cryst. (1987). B**43**, 448-454

Electron Density in Chromium Sulfate Pentahydrate

BY T. P. VAALSTA AND E. N. MASLEN

Crystallography Centre, University of Western Australia, Nedlands, Western Australia 6009, *Australia*

(*Received* 11 *September* 1986; *accepted* 1 *June* 1987)

Abstract

The structure of the title compound has been refined using an accurate set of X-ray data: $CrSO_4.5H_2O$, $M_r = 238{\cdot}1$, triclinic, $P\bar{1}$, $a = 6{\cdot}188\,(1)$, $b = 10{\cdot}929\,(2)$, $c = 6{\cdot}039\,(1)$ Å, $\alpha = 82{\cdot}40\,(2)$, $\beta = 107{\cdot}77\,(1)$, $\gamma = 102{\cdot}71\,(2)°$, $V = 378{\cdot}46\,(2)$ Å^3, $Z = 2$, $D_x = 2{\cdot}09$ g cm^{-3}, Mo $K\alpha$, $\lambda = 0{\cdot}71069$ Å, $\mu = 17{\cdot}03$ cm^{-1}, $F(000) = 244$, $T = 298$ K, $R = 0{\cdot}039$ for 7958 unique reflections. Difference electron-density maps are evaluated for sections through two Cr nuclei containing four water O atoms and ligating sulfate O atoms. The anisotropy of the deformation density $\Delta\rho$ around the Cr nuclei is related to unequal occupancy of the $3d$ metal orbitals, as expected in view of the Jahn-Teller distortion in the structure. The density

0108-7681/87/050448-07$01.50

along the Cr–O bonds is depleted less heavily than that along the Cu–O vectors in the nearly isostructural $CuSO_4.5H_2O$ structure. There is topological correspondence between the density maps for the two crystallographically independent Cr atoms. Differences between peak heights in the two maps reflect small changes in the structural geometry at the two sites. There is a correlation between the orientations of the features in the difference density near the Cr nuclei and the ligand water orientation.

Introduction

Analysis of the deformation of the electron density in transition-metal complexes with nearly ideal geometries was pioneered by Iwata & Saito (1973). Some complexes, studied to gain information on systems, such as metal–metal bonds, where the bonding mechanism was not clearly understood (Wang & Coppens, 1976; Mitschler, Rees & Lehmann, 1978), have less regular geometries.

In favourable cases, departures from ideal geometry may be exploited more systematically. It is often simpler to determine the relationship between the distortion in the structure and the departure from ideality in the density than it is to establish the relationship between the structure and the deformation density as a whole. Such a distortion exists in the γ-spinel structures M_2SiO_4 (M = Fe, Co and Ni) studied by Marumo, Isobe, Saito, Yagi & Akimoto (1974) and Marumo, Isobe & Akimoto (1977).

The series KMF_3, with M = Mn, Fe, Co and Ni, has the cubic perovskite structure (Kijima, Tanaka & Marumo, 1981, 1983; Miyata, Tanaka & Marumo, 1983). The structure of the Cu member of the series $KCuF_3$ has lower tetragonal symmetry because of the Jahn–Teller (1937) distortion of the ligand geometry around the Cu atom. The effect of this distortion on the electron density has been studied by Tanaka, Konishi & Marumo (1979) and by Tanaka & Marumo (1982).

To obtain a more detailed understanding of the relationship between the Jahn–Teller distortion and the electron density, Varghese & Maslen (1985) studied the deformation density in $CuSO_4.5H_2O$. That structure contains two crystallographically independent metal atoms, each coordinated to four water and two sulfate O atoms. The bonds from the Cu to the sulfate O atoms are elongated. The deformation density shows the effect of the distortion, the depletion of the electron density along the Cu–O vectors being less pronounced along the longer bonds.

The degree of the Jahn–Teller distortion differs for the two crystallographically independent Cu atoms. The characteristics of the deformation density around these atoms are correlated with the degree of distortion. Varghese & Maslen also noted changes in the deformation density along the different Cu–O bonds, which appeared to be associated with the orientation of the ligating water molecules.

Table 1. *Crystal and refinement data*

Crystal bounding planes	
Indices	D (mm)*
(100)	0·10
$\bar{1}00$)	0·10
($\bar{1}11$)	0·11
($1\bar{1}\bar{1}$)	0·10
($01\bar{1}$)	0·16
($0\bar{1}1$)	0·16
Diffractometer	Syntex $P2_1$ four-circle diffractometer
Scanning method	Conventional ω–2θ scan mode
Scan speed (°s^{-1}; min., max.)	0·081, 0·488
Number of scans	1
Max. variation in intensity of standard reflections [±700 ± 040 ± 005]	9%
Number of reflections measured	15 828
Number of unique reflections (n) ($-13 \le h \le 13$, $0 \le k \le 22$, $-13 \le l \le 13$)	7958
$(\sin\theta_{max})/\lambda$ (Å^{-1})	1·0805
Absorption correction range (min., max.)	1·33, 1·61
R_{int}	0·019
w	$1/\sigma^2(F)$
Number of parameters refined (m)	144
Largest shift	$0{\cdot}0010\sigma$
$S = [\sum w(\lvert F_o - F_c\rvert)^2/(N-m)]^{1/2}$	1·26
$R = \sum(\lvert F_o\rvert - \lvert F_c\rvert)/\sum\lvert F_o\rvert$	0·039
$wR = [\sum w(\lvert F_o\rvert - \lvert F_c\rvert)^2/\sum w\lvert F_o\rvert^2]^{1/2}$	0·049

* Distance from an internal origin.

The title compound is to a first approximation isostructural with $CuSO_4.5H_2O$. Geometrical details of the structure from an initial refinement are reported, along with an interpretation of the electronic spectrum by Hitchman, Lichon, McDonald, Smith, Stranger, Skelton & White (1987). There are some marked differences in detail between the structures, which provides the opportunity to study the relationship between the structural geometry and the electron density more closely. It also permits a study of the change in deformation density with the number of d electrons in a Jahn–Teller system.

Refinement of structure

Details of the measurement of the X-ray data for the charge density study are in Table 1. Cell dimensions were determined by least squares using six reflections with $55 < 2\theta < 60°$. Before averaging equivalents the measurements were corrected for absorption by an analytical method (Alcock, 1970). The slightly irregular crystal shape was approximated by the parallelepiped with the six planes listed, the linear absorption coefficient being evaluated from the mass absorption coefficients in *International Tables for X-ray Crystallography* (1962). Discrepancies between equivalents were scrutinized and corrected before averaging to give the unique set of reflections.

Structure factors were evaluated using the free-atom scattering factors for Cr, S, O and the spherical bonded-atom factor for H from *International Tables for X-ray Crystallography* (1962) with dispersion corrections from Cromer & Liberman (1970). The structure was refined by full-matrix least squares using the *XTAL* system program *SFLSX* (Stewart & Hall,

Table 2. *Atomic coordinates* ($\times 10^5$; $\times 10^4$ *for* H *atoms*) *and equivalent isotropic thermal parameters* ($Å^2 \times 10^2$)

$$U_{eq} = \frac{1}{6\pi^2} \sum_i \sum_j \beta_{ij} \mathbf{a}_i . \mathbf{a}_j .$$

	x	y	z	U_{eq}
Cr(1)	0	0	0	1·70
Cr(2)	$\frac{1}{2}$	$\frac{1}{2}$	0	1·45
S	1552 (3)	28735 (2)	−37115 (4)	1·44
O(1)	−9239 (13)	15604 (7)	−32044 (14)	2·52
O(2)	24640 (13)	31711 (7)	−20190 (14)	2·53
O(3)	−13304 (14)	37382 (8)	−36147 (13)	2·56
O(4)	4295 (14)	29897 (8)	39037 (12)	2·37
O(5)	−18451 (16)	7127 (9)	16590 (17)	2·93
O(6)	29565 (15)	12168 (7)	15655 (15)	2·66
O(7)	46513 (14)	40333 (9)	30648 (13)	2·71
O(8)	76140 (15)	41066 (10)	2085 (14)	3·79
O(9)	44003 (14)	12870 (9)	63248 (16)	2·93
H(54)	−1245 (35)	1282 (19)	2420 (34)	3·2 (5)
H(59)	−2597 (43)	355 (23)	2136 (41)	4·5 (6)
H(62)	3055 (42)	1883 (23)	804 (43)	5·6 (7)
H(69)	3550 (40)	1274 (21)	3306 (39)	4·5 (6)
H(73)	5787 (39)	3931 (19)	4214 (37)	4·0 (5)
H(74)	3470 (38)	3835 (19)	3141 (35)	3·7 (5)
H(83)	7994 (36)	4002 (19)	−619 (37)	3·2 (5)
H(84)	8330 (36)	3989 (19)	1235 (37)	3·3 (5)
H(91)	5735 (48)	1245 (25)	6876 (45)	6·1 (7)
H(92)	4155 (40)	1984 (21)	6797 (38)	4·0 (5)

1985). Positional parameters for S, O and H atoms, anisotropic temperature factors for all non-H atoms, isotropic temperature factors for the H atoms, and the scale factor were determined by minimizing $\sum w(|F_o| - |F_c|)^2$, where the weight for each reflection is the reciprocal of the variance in $|F_o|$. The variance is determined from counting statistics, but increased by an intensity-dependent term determined from the fluctuations in the standard reflections. The refinement indices, and the standard deviation of an observation of unit weight are included in Table 1. The structural parameters at the conclusion of the refinement are listed in Table 2.* Interatomic distances and angles are listed in Table 3.

Description of the structure

An *ORTEP* diagram (Johnson, 1965) of the structure is shown in Fig. 1. The notation is consistent with the tables and the numbering of the atoms is the same as that used by Beevers & Lipson (1934) for the isostructural $CuSO_4.5H_2O$. Cr(1) and Cr(2) occupy the non-equivalent special positions (0,0,0) and ($\frac{1}{2},\frac{1}{2},0$) respectively. The Cr(1) ion is surrounded by four sulfate groups, wth two S atoms at 3·660 (5) Å and two at 5·2052 (7) Å. Cr(2) has eight nearby S atoms, in pairs, at 3·6909 (4), 4·8510 (5), 5·4410 (6) and 5·5100 (7) Å.

* Lists of structure factors and anisotropic thermal parameters have been deposited with the British Library Document Supply Centre as Supplementary Publication No. SUP 44043 (28 pp.). Copies may be obtained through The Executive Secretary, International Union of Crystallography, 5 Abbey Square, Chester CH1 2HU, England.

Table 3. *Selected bond lengths* (Å) *and angles* (°) *for* $CrSO_4.5H_2O$ *with e.s.d.'s in parentheses*

(*a*) Hydrogen bonds to water molecules

	O···O	O–H	H···O	O–H···O
O(5)–H(54)–O(4)	2·863 (1)	0·78 (2)	2·09 (2)	170 (2)
O(5)–H(59)–O(9^{iii})	2·777 (1)	0·65 (3)	2·15 (2)	160 (3)
O(6)–H(62)–O(2)	2·829 (1)	0·81 (2)	2·06 (2)	159 (2)
O(6)–H(69)–O(9)	2·743 (1)	1·01(2)	1·74 (2)	176 (2)
O(7)–H(74)–O(4)	2·780 (1)	0·73 (2)	2·06 (2)	167 (2)
O(7)–H(73)–O(3^{i})	2·729 (1)	0·84 (2)	1·90 (2)	169 (3)
O(8)–H(83)–O(3^{ii})	2·684 (1)	0·65 (3)	2·05 (3)	170 (2)
O(8)–H(84)–O(4^{ii})	2·711 (1)	0·66 (2)	2·09 (2)	158 (3)
O(9)–H(91)–O(1^{i})	2·772 (1)	0·80 (3)	2·03 (3)	153 (3)
O(9)–H(92)–O(2^{iv})	3·006 (2)	0·91 (3)	2·14 (3)	159 (2)

(*b*) Angles at water O atoms

	O–O–O	H–O–H
H(54)–O(5)–H(59)	123·01 (5)	108 (3)
H(62)–O(6)–H(69)	131·06 (4)	115 (2)
H(74)–O(7)–H(73)	119·92 (4)	121 (2)
H(83)–O(8)–H(84)	107·24 (5)	111 (3)
H(91)–O(9)–H(92)	122·37 (4)	109 (2)

(*c*) Sulfate group

	O–S	S–O	O–S–O
O(1^{iv})–S^{i}–O(2^{iv})	1·4786 (8)	1·4777 (7)	109·10 (4)
O(1^{iv})–S^{i}–O(3^{iv})		1·4735 (10)	110·16 (5)
O(1^{iv})–S^{i}–O(4)		1·4868 (8)	108·43 (5)
O(2^{iv})–S^{i}–O(3^{iv})			111·16 (5)
O(2^{iv})–S^{i}–O(4)			108·86 (5)
O(3^{iv})–S^{i}–O(4)			109·08 (5)

(*d*) Cr–O bonds and selected angles

Bonds to SO_4^{2-} O atoms			
Cr(1)–O(1)	2·4209 (8)	Cr(2)–O(2)	2·4578 (8)
Bonds to water O atoms			
Cr(1)–O(5)	2·0518 (12)	Cr(2)–O(7)	2·0529 (8)
Cr(1)–O(6)	2·0532 (8)	Cr(2)–O(8)	2·0307 (11)
O(6)–Cr(1)–O(5)	89·43 (4)	O(7)–Cr(2)–O(8)	88·86 (4)

Symmetry code: none x, y, z; (i) $1+x, y, 1+z$; (ii) $1+x, y, z$; (iii) $-x, -y, 1-z$; (iv) $x, y, 1+z$.

The bond lengths and angles for the sulfate group are similar to those in $CuSO_4.5H_2O$ reported by Varghese & Maslen (1985). The average S–O bond length of 1·479 (1) Å for the title structure agrees with the

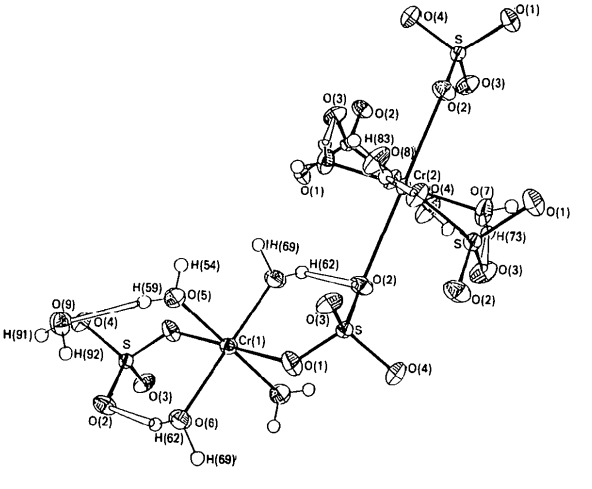

Fig. 1. An *ORTEP* (Johnson, 1965) drawing of the crystal structure of the title compound showing the bonding nature. Covalent and metal–O bonds are filled, O–H···O bonds are open.

value of 1·478 (1) Å found by Varghese & Maslen for $CuSO_4.5H_2O$. The differences in the S–O bond lengths are explained by the number of receptors for hydrogen bonds for each O atom. For example, the longest S–O bond [1·4868 (8) Å] involves O(4), which is the receptor for three hydrogen bonds, whereas O(1), O(2) and O(3) are receptors for two only.

There is a significant difference between the lengths of the Cr–O bonds to water O atoms and to the O atoms of the sulfate group, consistent with the Jahn–Teller (1937) effect. Within each type of Cr–O bond, however, there are significant differences such as that between Cr(1)–O(1) [2·4209 (8) Å] and Cr(2)–O(2) [2·4578 (8) Å]. Somewhat larger differences were observed for the $CuSO_4.5H_2O$ structure.

The coordination of both Cr atoms, with four water molecules and two sulfate O atoms as ligands, is similar, each having approximate 4/*mmm* symmetry as shown in Fig. 2. The metal–water O distances in $CrSO_4.5H_2O$ are longer than the corresponding Cu–O distances.

Whereas the proton positions for $CuSO_4.5H_2O$ reported by Varghese & Maslen (1985) were determined by neutron diffraction, the H-atom positions for the title compound were determined from this X-ray analysis. Their low scattering power limits the precision of the structural parameters for these H atoms, and their parameters also differ systematically from those of the protons because of the redistribution of the electrons due to chemical bonding. Nevertheless the precision of the results allows qualitative conclusions to be drawn.

The hydrogen-bonding network for Cr(1) differs from that of Cr(2). For the Cr(1) moiety the hydrogen bonds link to the space-filling waters and to O atoms of the ligating sulfate groups. This results in a near tetrahedral configuration of the water molecules (see Fig. 2(*a*). For Cr(2), the water H atoms link only to the O atoms of the surrounding sulfate groups.

As seen in Fig. 2(*b*), the water molecules around Cr(2) are in an approximately trigonal configuration

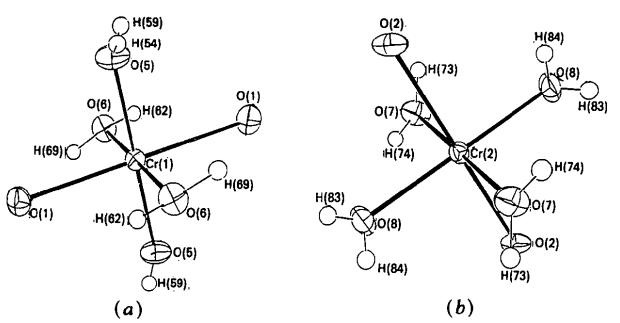

Fig. 2. An *ORTEP* (Johnson, 1965) view of the environment of the coordination sphere for the non-equivalent Cr atoms showing (*a*) the approximate tetrahedral configuration of the water molecules around Cr(1), and (*b*) the trigonal configuration of the water molecules around Cr(2). One H atom [H(54)] on O(5) is hidden by the O atom.

[type 1′ of Chiari & Ferraris (1982)]. The sums of the Cr(2)–O–H angles and H–O–H angles for the water ligands have values of 360 (5)° for the H(73)–O(7)–H(74) water ligand and 359 (7)° for the H(83)–O(8)–H(84) water ligand. Similar water ligands near Cu(2) in the $CuSO_4.5H_2O$ structure (Varghese & Maslen, 1985) have average H–O–H angles larger than those for the waters attached to Cu(1).

Around Cr(1) the configurations of the water molecules (defined by the two O–O vectors and Cr–O vectors) are intermediate between trigonal and tetrahedral [type 1 of Chiari & Ferraris (1982)], with the sum of the Cr(1)–O–H and H–O–H angles being 249 (5) and 350 (7)° for O(6) and O(5) respectively. This differs from the geometry for $CuSO_4.5H_2O$, where the water ligands around Cu(2) approximate a tetrahedral configuration more closely.

The mean H–O–H angle for the water molecules for the $CrSO_4.5H_2O$ structure is 113 (3)° compared with 109·7° for a trigonal angle and 105·9° for the tetrahedral angle for the structure classes 1 and 1′ of Chiari & Ferraris (1982). The mean value of the O···O···O angle is 120·7°, compared with 118·7° given by Chiari & Ferraris. The H–O–H angles are larger than the value for isolated water molecules in crystalline hydrates, as was observed in the $CuSO_4.5H_2O$ structure. The average opening of about 5° observed in this study can be attributed to a number of factors including the nature of the coordination bonds, the geometrical disposition of the hydrogen-bond acceptors, and the residual charge both on the H atoms and the molecules as a whole. Positive charges on H atoms repel each other, increasing the H–O–H angle.

However, Chiari & Ferraris (1982) report that the geometry of the coordination has the greatest influence on the opening of the H–O–H angle. Thus correlation between the H–O–H and O···O···O angles is due to the fact that the O–H···O hydrogen bonds favour linearity. In this structure this contributes to the enlargement of the H–O–H angle. The correlation between large O···O···O angle and large H–O–H angles in the hydrogen-bond network for O(5), O(6) and O(7) (see Table 3) is comparable to those for $CuSO_4.5H_2O$ reported in their Table 4 by Varghese & Maslen (1985).

Difference density

The ideal deformation density is the difference between the electron density in a crystal and that in a free-atom model with the same distribution function for the nuclei. Experimentally this is approximated by the difference density $\Delta\rho$, obtained by Fourier transformation from the set of $F_o/k - F_c$ values, where k is the scale factor, F_c is calculated with spherical free-atom form factors, and F_o is corrected for dispersion.

Sections of the deformation density for each of the six planes containing a metal atom and four ligating O atoms are shown in Fig. 3. $\sigma(\Delta\rho)$, the point estimate of the accuracy of $\Delta\rho$, estimated as described by Davis & Maslen (1978), is 0·06 e Å^{-3}. It is not obvious how to relate the significance of the features in the difference density to this point estimate. An alternative guide to precision is given by the internal consistency of maps containing atoms in chemically similar arrangements.

There is a strong resemblance between the maps in Figs. 3(*a*), (*b*) and (*c*), containing Cr(1), and the corresponding maps 3(*d*), (*e*) and (*f*), containing Cr(2). There is less difference between these than there is between the corresponding maps for $CuSO_4.5H_2O$. This is consistent with the closer correspondence between the environments of the two metal atoms in the $CrSO_4.5H_2O$ structure. Furthermore, the more significant differences between the $\Delta\rho$ maps correlate with differences in the structural geometry. For example, the electron density near Cr accumulates along the longer Cr–O vectors directed towards the sulfate O atoms. The peak height is larger (0·5 e Å^{-3}) along the Cr(2)–O(2) bond than the value of 0·25 e Å^{-3} for the Cr(1)–O(1) bond. The lengths of these bonds are 2·4578 (8) and 2·4209 (8) Å respectively. There is strong depletion of density along Cr(2)–O(8) which is the shortest of the bonds to the ligating waters. The shapes of the depleted regions for the bonds of intermediate length are more complex, and cannot be classified in terms of peak height only.

The depletion of density near the metal atom is less marked than that of the electron density near the Cu atom in $CuSO_4.5H_2O$. This result is consistent with the *d* subshell populations in the two cases. With the close approach of an electron-rich O-ligand atom the *d* subshell of Cu is heavily depleted of density due to exchange. For Cr, with a half-filled *d* subshell, the depletion of the density is less severe.

The topography of the deformation density near the Cr atoms is qualitatively consistent with an orbital description of the Jahn–Teller theorem. The depletion of density in the plane containing the water O atoms is associated with a hole in the $d_{x^2-y^2}$ orbital created when the d^5 configuration of the Cr atom changes to the d^4 configuration of the Cr^{2+} free ion.

The positive peaks observed on the Cr–sulfate O bonds (Figs. 3*b*, *c*, *e*, *f*), indicate movement of electrons into the $3d_{z^2}$ orbital, lengthening the Cr–sulfate

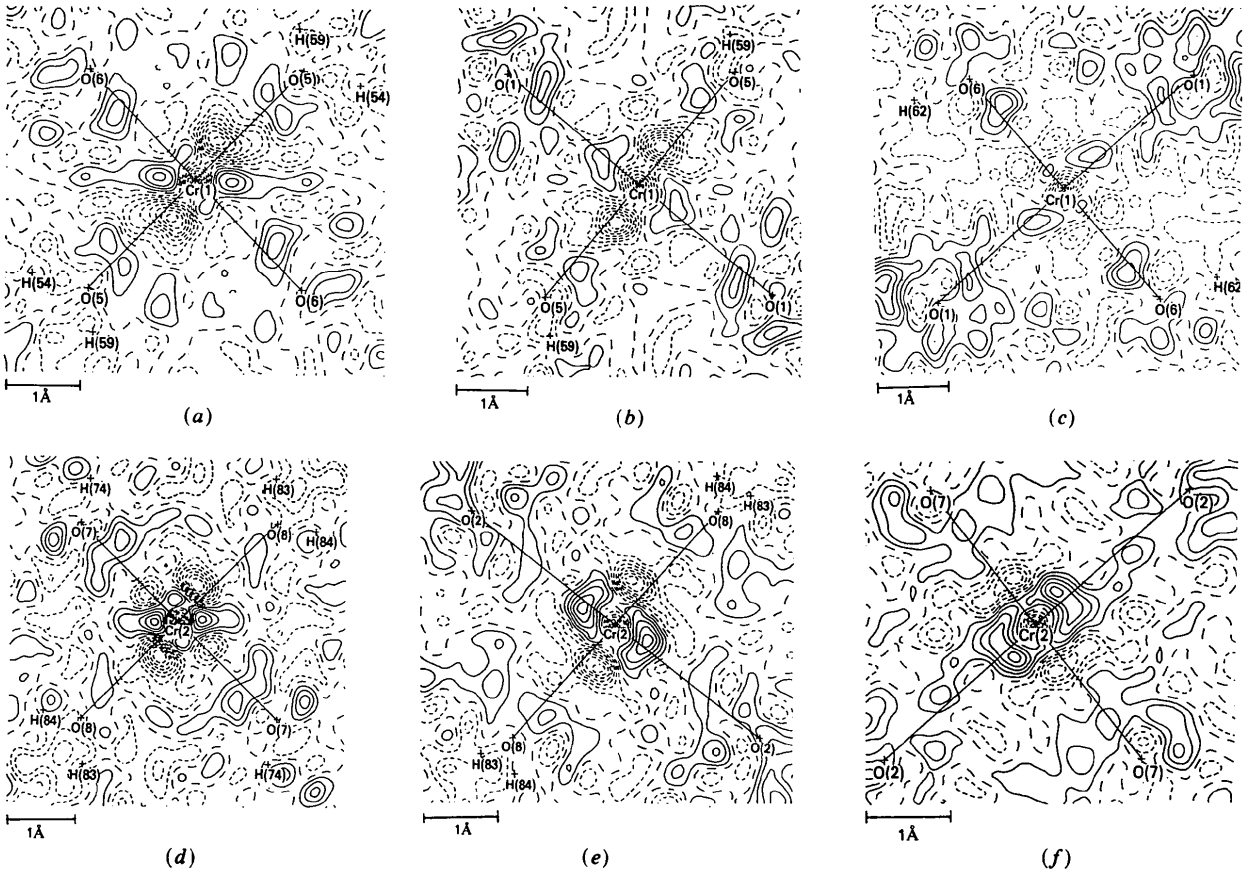

Fig. 3. Difference density maps for sections containing (*a*) Cr(1), O(5) and O(6); (*b*) Cr(1), O(5) and O(1); (*c*) Cr(1), O(6) and O(1); (*d*) Cr(2), O(8) and O(7); (*e*) Cr(2), O(8) and O(2); (*f*) Cr(2), O(2) and O(7). The contour interval is 0·1 e Å^{-3}.

O bond. These positive peaks are slightly displaced from the line of the Cr–sulfate O vector. This twisting of the peaks from Cr–O bond location correlates with the orientation of the ligand water molecules above and perpendicular to these planes. The correlation is particularly strong for Cr(2), where the water ligands are trigonal. The H–O vectors for the ligand waters above and below maps 3(*e*) and 3(*f*) were projected onto those planes. The projected vectors lie along the line joining the three minima at and adjacent to Cr(2), with the peaks lying on opposite sides of the projected H–O–H line. The topography of the maps indicates that the geometry of the ligand water molecules has a strong influence on the electron-density distribution. The correlation is less strong for Cr(1), for which the water ligand configurations are intermediate between tetrahedral and trigonal, but the twisting behaviour is still observable. The poorer correlation is expected, since the H–O–H molecule does not appear linear in orientation in the planes parallel to Figs. 3(*b*) and (*c*). Varghese & Maslen (1985) also noted significant changes in the topography of the deformation density along the Cu–O bonds for $CuSO_4.5H_2O$ that correlated with the orientations of the ligating water molecules.

There are peaks around the Cr atoms in spaces avoiding the ligands (see Figs. 3*a*, *d*). The peaks are close to the metal, of height 0·4 e Å^{-3} at 0·50 Å and of height 0·1 e Å^{-3} at 0·41 Å for Cr(1), with larger peaks of height 0·5 e Å^{-3} at 0·35 Å and 0·2 e Å^{-3} at a distance of 0·32 Å for Cr(2). These peaks are associated with increased occupancy of the $3d_{xy}$ orbital. The features resemble qualitatively the results of Johansen (1976), whose difference densities for three transition-metal complexes, calculated theoretically, showed pronounced deformation peaks near the metal atoms and directed away from the ligands.

In order to investigate the relationship between charge and geometry in the $CrSO_4.5H_2O$ structure, the charges of the atoms in this structure were calculated by electron-density partitioning, using the overlapping pseudoatom scheme of Hirshfeld (1977) implemented *via* the program *PARTN* (Chantler, 1985). For comparison, similar calculations were performed on the isostructural compound $CuSO_4.H_2O$. In order to assess the importance of the H-atom coordinates on the estimated charges, these were calculated using both X-ray and neutron parameters for the $CuSO_4.5H_2O$ structure. The e.s.d.'s in the charges were calculated as described by Davis & Maslen (1978). The results are given in Table 4. The effects of the change from neutron to X-ray parameters for $CuSO_4.5H_2O$ are not significant.

On comparing the columns in Table 4 for the group charges for the $CrSO_4.5H_2O$ and $CuSO_4.5H_2O$ structures, close similarities are noted. The correspondence between the charges for groups is closer than that for individual atoms. The charges on the space-

Table 4. *Atomic and group charges obtained from the partitioning scheme of Hirshfeld* (1977)

Estimated standard deviations calculated by the method of Davis & Maslen (1978).

	$CrSO_4.5H_2O$ structure X-ray parameters		$CuSO_4.5H_2O$ structure X-ray parameters	Neutron parameters
(*a*) Atomic charges (e)				
Cr(1)	0·76 (9)	Cu(1)	0·24 (4)	0·22 (4)
Cr(2)	0·16 (9)	Cu(2)	0·28 (4)	0·28 (4)
S	0·24 (6)	S	0·06 (2)	0·06 (2)
O(1)	−0·41 (6)	O(1)	−0·45 (2)	−0·48 (2)
O(2)	−0·24 (6)	O(2)	−0·39 (2)	−0·38 (2)
O(3)	−0·20 (6)	O(3)	−0·22 (2)	−0·23 (2)
O(4)	−0·36 (6)	O(4)	−0·20 (2)	−0·22 (2)
O(5)	−0·03 (6)	O(5)	0·25 (2)	0·22 (2)
O(6)	−0·01 (6)	O(6)	−0·04 (2)	−0·06 (2)
O(7)	−0·06 (6)	O(7)	0·04 (2)	0·02 (2)
O(8)	0·06 (6)	O(8)	0·02 (2)	0·09 (2)
O(9)	−0·10 (6)	O(9)	−0·08 (2)	−0·03 (2)
H(54)	0·01 (4)	H(54)	0·04 (2)	0·05 (2)
H(59)	0·01 (4)	H(59)	0·16 (2)	0·17 (2)
H(62)	0·07 (4)	H(62)	0·04 (2)	0·06 (2)
H(69)	0·12 (4)	H(69)	0·06 (2)	0·07 (2)
H(73)	0·09 (4)	H(73)	0·03 (2)	0·04 (2)
H(74)	−0·01 (4)	H(74)	0·09 (2)	0·08 (2)
H(83)	0·08 (4)	H(83)	0·16 (2)	0·15 (2)
H(84)	0·08 (4)	H(84)	0·03 (2)	0·01 (2)
H(91)	0·04 (4)	H(91)	0·10 (2)	0·05 (2)
H(92)	0·15 (4)	H(92)	0·03 (2)	0·08 (2)
(*b*) Group charges (e)				
SO_4^{2-}	−0·97 (13)	SO_4^{2-}	−1·20 (4)	−1·25 (4)
H–O(5)–H	−0·01 (8)	H–O(5)–H	0·45 (3)	0·44 (3)
H–O(6)–H	0·18 (8)	H–O(6)–H	0·06 (3)	0·07 (3)
H–O(7)–H	0·02 (8)	H–O(7)–H	0·16 (3)	0·14 (3)
H–O(8)–H	0·22 (8)	H–O(8)–H	0·21 (3)	0·25 (3)
H–O(9)–H	0·09 (8)	H–O(9)–H	0·05 (3)	0·10 (3)
$Cr(1).2H_2O(5).2H_2O(6)$	1·1 (2)	$Cu(1).2H_2O(5).2H_2O(6)$	1·26 (7)	1·24 (7)
$Cr(2).2H_2O(7).2H_2O(8)$	0·7 (2)	$Cu(2).2H_2O(7).2H_2O(8)$	1·02 (7)	1·06 (7)
Unit-cell total	0·0 (2)	Unit-cell total	0·0 (1)	0·0 (1)

filling water molecule $H_2O(9)$ for both structures are consistent, as expected from the similarity in the environments for these water molecules in the two structures. The charge on the $Cr(1).2H_2O(5).2H_2O(6)$ moiety [1·1 (2) e] is larger than that of the $Cr(2).2H_2O(7).2H_2O(8)$ moiety [0·7 (2) e]. The same relationship is observed for the $CuSO_4.5H_2O$ structure. The charge on the $Cu(1).2H_2O(5).2H_2O(6)$ moiety [1·24 (7) e] is larger than that on $Cu(2).2H_2O(7).2H_2O(8)$ [1·06 (7) e]. The ligating water molecules for both structures have residual charges that are slightly positive or neutral. The SO_4^{2-} groups have negative charges of similar magnitude in both structures. These global similarities reflect the isostructural and isochemical properties of $CrSO_4.5H_2O$ and $CuSO_4.5H_2O$.

The differences in the magnitudes of the charges of the moiety groups for $CrSO_4.5H_2O$ and $CuSO_4.5H_2O$ are consistent with the differences in the strength of the electrostatic interaction between the central transition metals and the ligand O atoms, noting the larger influence of the Jahn–Teller effect on the $CuSO_4.5H_2O$ structure. In $CuSO_4.5H_2O$, the charge for the sulfate moiety [−1·25 (4) e] is somewhat larger than that for $CrSO_4.5H_2O$ [−1·0 (1) e]. The mean ligand water molecule charge of 0·32 (2) e and the charge of the $Cu.4H_2O$ moieties [1·24 (7) for

Cu(1) and 1·06 (7) e for Cu(2)] are greater than the corresponding values for $CrSO_4.5H_2O$ [a mean value of 0·10 (4) e for the ligating water molecules, and 1·1 (2) and 0·7 (2) e for the $Cr(1).4H_2O$ and $Cr(2).4H_2O$ moieties respectively].

The average charges on the sulfate O atoms are comparable for the two structures, being −0·30 (3) e for $CrSO_4.5H_2O$ and −0·32 (1) e for $CuSO_4.5H_2O$. However, the agreement between the individual charges on the sulfate O atoms does not compare so favourably, indicating a need for caution when interpreting individual charges.

Calculations were performed on a Perkin-Elmer 3240 computer using programs from the *XTAL* system (Stewart & Hall, 1985). We thank C. Chantler for use of the program *PARTN*, which is compatible with the *XTAL* system. We also thank B. W. Skelton for providing the X-ray data.

References

ALCOCK, N. W. (1970). *Crystallographic Computing*, edited by F. R. AHMED, pp. 271-278. Copenhagen: Munksgaard.
BEEVERS, C. H. & LIPSON, H. (1934). *Proc. R. Soc. London Ser. A*, **146**, 570-582.
CHANTLER, C. (1985). *PARTN* program-listing and documentation. Unpublished.
CHIARI, G. & FERRARIS, G. (1982). *Acta Cryst.* B**38**, 2331-2341.
CROMER, D. T. & LIBERMAN, D. (1970). *J. Chem. Phys.* **53**, 1891-1898.
DAVIS, C. L. & MASLEN, E. N. (1978). *Acta Cryst.* A**34**, 743-746.
HIRSHFELD, F. L. (1977). *Theor. Chim. Acta*, **44**, 129-138.
HITCHMAN, M. A., LICHON, M., MCDONALD, R. G., SMITH, P. W., STRANGER, R., SKELTON, B. W. & WHITE, A. H. (1987). *J. Chem. Soc. Dalton Trans.* In the press.
International Tables for X-ray Crystallography (1962). Vol. III. Birmingham: Kynoch Press. (Present distributor D. Reidel, Dordrecht.)
IWATA, M. & SAITO, Y. (1973). *Acta Cryst.* B**29**, 822-832.
JAHN, H. A. & TELLER, E. (1937). *Proc. R. Soc. London Ser. A*, **161**, 220-235.
JOHANSEN, H. (1976). *Acta Cryst.* A**32**, 353-355.
JOHNSON, C. K. (1965). *ORTEP*. Report ORNL-3794. Oak Ridge National Laboratory, Tennessee, USA.
KIJIMA, N., TANAKA, K. & MARUMO, F. (1981). *Acta Cryst.* B**37**, 545-548.
KIJIMA, N., TANAKA, K. & MARUMO, F. (1983). *Acta Cryst.* B**39**, 557-561.
MARUMO, F., ISOBE, M. & AKIMOTO, S. (1977). *Acta Cryst.* B**33**, 713-716.
MARUMO, F., ISOBE, M., SAITO, Y., YAGI, T. & AKIMOTO, S. (1974). *Acta Cryst.* B**30**, 1904-1906.
MITSCHLER, A., REES, B. & LEHMANN, M. S. (1978). *J. Am. Chem. Soc.* **100**, 3390-3397.
MIYATA, N., TANAKA, K. & MARUMO, F. (1983). *Acta Cryst.* B**39**, 561-564.
STEWART, J. M. & HALL, S. R. (1985). *The XTAL System of Crystallographic Programs. User's Manual.* Computer Science Center, Univ. of Maryland, College Park, Maryland, USA.
TANAKA, K., KONISHI, M. & MARUMO, F. (1979). *Acta Cryst.* B**35**, 1303-1308.
TANAKA, K. & MARUMO, F. (1982). *Acta Cryst.* B**38**, 1422-1427.
VARGHESE, J. N. & MASLEN, E. N. (1985). *Acta Cryst.* B**41**, 184-190.
WANG, Y. & COPPENS, P. (1976). *Inorg. Chem.* **15**, 1122-1127.

Acta Cryst. (1987). B**43**, 454-456

Ionic Radii and Optical Susceptibilities in the Halite-Type Alkali Halides

BY W. KUCHARCZYK

Institute of Physics, Technical University, ul. Wólczańska 219, 93-005 *Łódź, Poland*

(*Received* 8 *December* 1986; *accepted* 2 *June* 1987)

Abstract

The ionic radii providing the observed optical susceptibilities in alkali halides have been determined. The result is the set of crystal radii $r_a \simeq 0{\cdot}78$, 0·91, 0·92, 0·98, 1·08, 1·20, 1·24, 1·32, 1·31, 1·51, 1·61, 1·66, 1·40, 1·66, 1·73 and 1·82 Å and $r_h \simeq 1{\cdot}23$, 1·66, 1·83, 2·02, 1·23, 1·62, 1·75, 1·92, 1·37, 1·64, 1·69, 1·87, 1·43, 1·64, 1·71 and 1·85 Å for LiF, LiCl, LiBr, LiI, NaF, NaCl, NaBr, NaI, KF, KCl, KBr, KI, RbF, RbCl, RbBr and RbI, respectively. The calculations were performed at an assumed constant compensation coefficient related to the deficiency of the free-electron model.

Theory

The Phillips-Van Vechten theory of dielectric properties of solids (Phillips, 1968; Phillips & Van Vechten, 1969; Van Vechten, 1969) and the bond-charge model (Levine, 1973*a*,*b*) are the basis of numerous calculations of diverse optical phenomena (see *e.g.* Chemla, 1980; Shih Chun-Ching & Yariv, 1982; Tsirelson, Korolkova, Rez & Ozerov, 1984; Kucharczyk, 1987*a*; Sangwal & Kucharczyk, 1987). The starting point for all the calculations is Penn's nearly-free-electron model of the dielectric constant at long wavelengths (Penn, 1962)

$$\varepsilon(\infty) - 1 = (\hbar\omega_P / E_g)^2, \qquad (1)$$

0108-7681/87/050454-03$01.50